

## Guest-Tuned Spin Crossover in a Flexible $[X \subset [FeL_3]_2]^{3+}$ ( $X^- = Cl^-, Br^-, I^-$ ) Supramolecular Assembly.

M. D. Darawsheh,<sup>a</sup> L. A. Barrios<sup>a</sup>, O. Roubeau<sup>b</sup>, S. J. Teat<sup>c</sup> and G. Aromí<sup>\*a</sup>

### SUPPORTING INFORMATION

#### Synthesis

The ligand 1,3-bis(3-(pyridin-2-yl)-1H-pyrazol-5-yl)benzene, L, was prepared according to a procedure recently published by us.<sup>[1]</sup> All reactions were performed in air.

**(Cl@[FeL<sub>3</sub>]<sub>2</sub>)(OH)(PF<sub>6</sub>)<sub>2</sub>·H<sub>2</sub>O (1·H<sub>2</sub>O).** A suspension of L (25 mg, 0.069 mmol) in methanol (7 mL) was added dropwise to a methanolic solution (3 mL) of FeCl<sub>2</sub>·4H<sub>2</sub>O (9.1 mg, 0.046 mmol). The resulting red solution was stirred for 45 minutes and then filtered. The filtrate was layered with a solution of NH<sub>4</sub>PF<sub>6</sub> (7.5 mg, 0.046 mmol) in water (10 ml), producing red crystals after a few days. The yield of crystals was 3.6 mg (12.1 %), while the remaining powder was discarded. Crystals were separated cleanly using a pipette, and dried in air. *Anal.* Calc. (Found) for **1** 2H<sub>2</sub>O·5CH<sub>3</sub>OH: C, 57.82 (58.23); H, 4.32 (3.91); N, 17.72 (17.32). ESI-MS (m/z, M<sup>n+</sup>): 777.19, [Fe(H<sub>2</sub>L4)<sub>3</sub>Fe(H<sub>2</sub>L4)<sub>3</sub>Cl]<sup>3+</sup>; 1147.37, [Fe(H<sub>2</sub>L4)<sub>3</sub>Fe(HL4)<sub>3</sub>]<sup>2+</sup>; 1165.86, [Fe(H<sub>2</sub>L4)<sub>3</sub>Fe(H<sub>2</sub>L4)<sub>2</sub>(HL4)Cl]<sup>2+</sup>; 1196.8, [Fe(H<sub>2</sub>L4)<sub>3</sub>Fe(H<sub>2</sub>L4)<sub>3</sub>PF<sub>6</sub>]<sup>2+</sup>; 1220.8, [Fe(H<sub>2</sub>L4)<sub>3</sub>Fe(H<sub>2</sub>L4)<sub>2</sub>(HL4)PF<sub>6</sub>]<sup>2+</sup>; 1239.36, [Fe(H<sub>2</sub>L4)<sub>3</sub>Fe(H<sub>2</sub>L4)<sub>3</sub>CIPF<sub>6</sub>]<sup>2+</sup>.

**(Br@[FeL<sub>3</sub>]<sub>2</sub>)(OH)(PF<sub>6</sub>)<sub>2</sub>·H<sub>2</sub>O (2·H<sub>2</sub>O).** A suspension of L (25 mg, 0.069 mmol) in methanol (7 mL) was added dropwise to a solution of FeBr<sub>2</sub> (13.5 mg, 0.046 mmol) in methanol (3 mL). The resulting red solution was stirred for 45 minutes and then filtered. The filtrate was layered with a solution of NH<sub>4</sub>PF<sub>6</sub> (7.5 mg, 0.046 mmol) in water (10 mL), producing red crystals after a few days. The yield of crystals was 3.9 mg (12.5 %), while the remaining powder was discarded. Crystals were separated cleanly using a pipette, and dried in air. *Anal.* Calc. (Found) for **2**·8H<sub>2</sub>O: C, 55.69(55.27); H, 4.07 (3.65); N, 17.71 (17.35). ESI-MS (m/z, M<sup>n+</sup>): 1147.37, [Fe(H<sub>2</sub>L4)<sub>3</sub>Fe(HL4)<sub>3</sub>]<sup>2+</sup>.

**(I@[FeL<sub>3</sub>]<sub>2</sub>)(PF<sub>6</sub>)<sub>2.23</sub>·0.21(I<sub>3</sub>)<sub>0.56</sub> (3·2CH<sub>3</sub>OH).** A suspension of L (25 mg, 0.069 mmol) in methanol (20 mL) was added dropwise to a solution of FeI<sub>2</sub> (14.3 mg, 0.046 mmol) in methanol (5 mL). The resulting red solution was stirred for 45 minutes and then filtered. The filtrate was treated with a solution of NH<sub>4</sub>PF<sub>6</sub> (7.5 mg, 0.046 mmol) in methanol (5 mL) and the mixture was then left for slow evaporation at ambient temperature, which yielded red crystals after a few days. Crystals were separated cleanly by filtration. The yield of

crystals was 2.5 mg (7.1%). *Anal. Calc.* (Found) for  $3 \cdot 2\text{CH}_3\text{OH} \cdot 2\text{H}_2\text{O}$ : C, 52.11(51.82); H, 3.52 (3.34); N, 16.33 (16.43).

**(I@[FeL<sub>3</sub>]<sub>2</sub>)I<sub>2</sub>(I<sub>3</sub>)<sub>0.6</sub>(OH)<sub>0.4</sub>·0.6H<sub>2</sub>O·2CH<sub>3</sub>OH·2C<sub>3</sub>H<sub>6</sub>O (4·0.6H<sub>2</sub>O·2CH<sub>3</sub>OH·2C<sub>3</sub>H<sub>6</sub>O).** A suspension of L (25 mg, 0.069 mmol) in methanol (10 mL) was added dropwise to a solution of Fe(CF<sub>3</sub>SO<sub>3</sub>)<sub>2</sub>·6H<sub>2</sub>O (10.4 mg, 0.023 mmol) in methanol (5 mL). The resulting red solution was stirred for 30 minutes and then filtered. A solution with 5-fold excess of NBu<sub>4</sub>I (0.085 mg, 0.23 mmol) in methanol (5 mL) was then added, yielding a heavy precipitate. The solid was collected by filtration and then dissolved in hot nitromethane. The resulting red solution was allowed to cool to room temperature and vapors of ethylacetate were then allowed to diffuse in, yielding red crystals after few days. The yield of crystals was 1.5 mg (4.2 %). Crystals were separated cleanly using a pipette, and dried in air. *Anal. Calc.* (Found) for  $4 \cdot 0.6\text{H}_2\text{O} \cdot 2\text{C}_3\text{H}_6\text{O}$ : C, 54.50 (54.62); H, 3.63 (3.51); N, 16.58 (16.97).

**(Cl@[FeL<sub>3</sub>]<sub>2</sub>)(FeCl<sub>4</sub>)<sub>3</sub>·2C<sub>3</sub>H<sub>6</sub>O·4C<sub>7</sub>H<sub>8</sub> (5·2C<sub>3</sub>H<sub>6</sub>O·4C<sub>7</sub>H<sub>8</sub>).** A suspension of L (25 mg, 0.069 mmol) in acetone (10 mL) was added dropwise to a solution of FeCl<sub>2</sub>·4H<sub>2</sub>O (13.6 mg, 0.069 mmol) in acetone (5 mL). The resulting red solution was stirred for 1 hour and then filtered. The filtrate was layered with toluene producing red crystals after a few days. The yield of crystals was 1.6 mg (3.4 %). Crystals were separated cleanly using a pipette, and dried in air. *Anal. Calc.* (Found) for  $5 \cdot 3\text{H}_2\text{O} \cdot 2\text{C}_3\text{H}_6\text{O} \cdot \text{C}_7\text{H}_8$ : C, 54.61 (54.40); H, 3.86 (3.59); N, 15.81 (15.62).

### Physical Measurements

Variable-temperature magnetic susceptibility data were obtained with a MPMS-XL SQUID magnetometer at the Unitat de Mesures Magnètiques of the Universitat de Barcelona on polycrystalline samples used immediately after being removed from their mother liquor. Elemental analyses were performed with an Elemental Microanalyzer (A5), model Flash 1112 at the Servei de Microanàlisi of CSIC, Barcelona, Spain on samples that had been exposed in air of several hours. IR spectra were recorded as KBr pellet samples on a Nicolet AVATAR 330 FTIR spectrometer. Positive ion ESI TOF mass spectrometry experiments were performed on a LC/MSD-TOF (Agilent Technologies) at the Unitat d'Espectrometria de Masses de Caracterització Molecular (CCiT) of the University of Barcelona. The experimental parameters were: capillary voltage 4 kV, gas temperature 325°C, nebulizing gas pressure 15 psi, drying gas flow 7.0 L min<sup>-1</sup>, and fragmentor voltage ranging from 175 to 300 V. Samples (μL) were introduced into the source by a HPLC system (Agilent 1100), using a mixture of H<sub>2</sub>O/MeCN (1/1) as eluent (200 μL min<sup>-1</sup>). <sup>1</sup>H NMR spectra were recorded on a Bruker AVQ Spectrometer (400 MHz) or a Varian Mercury Spectrometer (400 MHz) at the Unitat de RMN of the Universitat de Barcelona. The spectra were collected using an "inset" tube inside the

sample tube in order to determine the chemical shift of the reference TMS in the solvent of the experiment without the influence of the paramagnetic material.

### Single Crystal X-ray Diffraction (SCXRD).

Data for compounds **1-5** were collected at 100 K on Beamline 11.3.1 at the Advanced Light Source, on a Bruker D8 diffractometer equipped with a PHOTON 100 CCD detector and using silicon 111 monochromated synchrotron radiation ( $\lambda = 0.7749 \text{ \AA}$ ). The crystals were mounted on a MiTegen kapton loop and placed in the  $N_2$  stream of an Oxford Cryosystems Cryostream Plus.

For **1-4**, data reduction and absorption corrections were performed with SAINT and SADABS, respectively.<sup>[2]</sup> All structures were solved by intrinsic phasing with SHELXT<sup>[3]</sup> and refined by full-matrix least-squares on  $F^2$  with SHELXL-2014.<sup>[4]</sup> In the structures of **1** and **2**, for charge balance and as reflected on the formula, the oxygen site O1 is shared by a water molecule and a hydroxide ion, and the hydrogen on O1 was thus refined with 1/2 occupancy. In the structure of **3**, The three  $PF_6^-$  anions are disordered with either an  $I_3^-$  anion (P2 and P3) or an  $I^-$  anion (P1), sharing the same space, with relative occupancies of respectively 0.79:0.21 for P1:I2, 0.692:0.308 for P2:(I3-I4-I5) and 0.75:0.15:0.10 for P3:(I6-I7-I8):(I9-I10-I11). In the structure of **4**, the  $I_3^-$  anion (atom sites I3 and I4) is partially occupied (0.6) and the missing charge is compensated by the oxygen O1 being either a hydroxide (0.4) or a water molecule (0.6).

Crystals of **5** were found to be twinned upon inspection of the data in RLATT.<sup>[2]</sup> The twinning was treated with CELL\_NOW.<sup>[5]</sup> The twin law was found to be a rotation by 180 degrees about (real) axis 1.000 0.093 0.071. Cell refinement and integration were then performed by SAINT<sup>[2]</sup> as a 2-component twin, keeping the cell of both components identical. TWINABS<sup>[5]</sup> was used for absorption corrections and produced HKLF4 and HKLF5 data, respectively for initial structure solution and refinement and final refinement.

All details can be found in CCDC 1512924 (**1**), 1512927 (**2**), 1512928 (**3**), 1512926 (**4**), and 1512925 (**5**), that contain the supplementary crystallographic data for this paper. These data can be obtained free of charge from The Cambridge Crystallographic Data Centre via <https://summary.ccdc.cam.ac.uk/structure-summary-form>. Crystallographic and refinement parameters are summarized in Table S1. Selected bond lengths and angles and intermolecular distances are given in Tables S2 and S3.

### References:

- [1] M. Darawsheh, L. A. Barrios, O. Roubeau, S. J. Teat, G. Aromí, *Chem., Eur. J.* **2016**, *22*, 8635-8645.
- [2] SAINT, RLATT and SADABS, Bruker AXS Inc., Madison, Wisconsin, USA.
- [3] G. M. Sheldrick, *Acta Cryst. A* **2015**, *71*, 3-8.
- [4] G. M. Sheldrick, *Acta Cryst. C* **2015**, *71*, 3-8.
- [5] CELL\_NOW and TWINABS, Bruker AXS Inc., Madison, Wisconsin, USA.



**Table S1.** Crystal data for compounds **1-5**.

Compound	<b>1</b>	<b>2</b>	<b>3</b>	<b>4</b>	<b>5</b>
Crystal size (mm <sup>3</sup> )	0.20x0.20x0.01	0.13x0.09x0.01	0.25x0.08x0.02	0.10x0.05x0.01	0.32x0.18x0.16
Formula	2(C <sub>66</sub> H <sub>48</sub> FeN <sub>18</sub> ), 2(PF <sub>6</sub> ), Cl, (H <sub>2</sub> O), (HO)	2(C <sub>66</sub> H <sub>48</sub> FeN <sub>18</sub> ), 2(PF <sub>6</sub> ), Br, (H <sub>2</sub> O), (HO)	2(C <sub>66</sub> H <sub>48</sub> FeN <sub>18</sub> ), 2.23(PF <sub>6</sub> ), 1.21(I), 0.56(I <sub>3</sub> ), 2(CH <sub>4</sub> O)	2(C <sub>66</sub> H <sub>48</sub> Fe N <sub>18</sub> ), 2(C <sub>3</sub> H <sub>6</sub> O), 2(CH <sub>4</sub> O), 3I, 0.6(I <sub>3</sub> ), 0.8(HO), 1.2(H <sub>2</sub> O)	2(C <sub>66</sub> H <sub>48</sub> FeN <sub>18</sub> ), 3(FeCl <sub>4</sub> ), 4(C <sub>7</sub> H <sub>8</sub> ), 2(C <sub>3</sub> H <sub>6</sub> O), Cl
FW (g mol <sup>-1</sup> )	2658.56	2703.02	3051.93	3126.77	3411.23
Wavelength (Å)	0.7749	0.7749	0.7749	0.7749	0.7749
Crystal system	trigonal	trigonal	monoclinic	monoclinic	triclinic
Space group	<i>P</i> -3c1	<i>P</i> -3c1	<i>P</i> 2 <sub>1</sub> / <i>n</i>	<i>C</i> 2/ <i>c</i>	<i>P</i> -1
Z	2	2	4	4	2
T (K)	100(2)	100(2)	100(2)	100(2)	100(2)
<i>a</i> (Å)	13.4555(8)	13.5619(5)	24.3560(10)	23.9867(8)	13.4928(6)
<i>b</i> (Å)	13.4555(8)	13.5619(5)	13.6794(7)	13.4513(5)	21.3643(10)
<i>c</i> (Å)	37.438(3)	37.307(2)	39.437(2)	40.6047(14)	28.7728(13)
<i>A</i> (°)	90	90	90	90	73.320(3)
<i>B</i> (°)	90	90	97.682(3)	91.448(2)	80.537(3)
<i>C</i> (°)	120	120	90	90	85.230(3)
<i>V</i> (Å <sup>3</sup> )	5870.1(8)	5942.4(5)	13021.5(11)	13097.0(8)	7831.4(6)
$\rho_{\text{calcd}}$ (g cm <sup>-3</sup> )	1.504	1.511	1.557	1.586	1.447
$\mu$ (mm <sup>-1</sup> )	0.487	0.867	1.274	1.778	0.933
Independent reflections	1230	4960	18863	13380	34424
restraints / parameters	269 / 285	1 / 285	536 / 1861	40 / 889	434 / 2057
Goodness-of-fit on <i>F</i> <sup>2</sup>	1.099	1.150	1.060	1.099	1.052
Final <i>R</i> <sub>1</sub> / <i>wR</i> <sub>2</sub> [ <i>I</i> > 2σ( <i>I</i> )]	0.1402 / 0.3014	0.0651 / 0.1644	0.1231 / 0.3389	0.0844 / 0.2120	0.0805 / 0.1812
Final <i>R</i> <sub>1</sub> / <i>wR</i> <sub>2</sub> [all data]	0.1589 / 0.3137	0.0764 / 0.1725	0.1547 / 0.3705	0.1096 / 0.2253	0.1300 / 0.2130
largest diff. peak and hole (e Å <sup>3</sup> )	0.673 / -0.363	1.416 / -1.090	2.747 / -3.424	1.387 / -3.425	1.176 / -1.339

**Table S2.** Fe–N bond lengths and Fe⋯Fe and Fe⋯X separations within the supramolecular (X@[FeL<sub>3</sub>]<sub>2</sub>)<sup>3+</sup> unit (Å) in the structure of compounds **1-5**.

<b>1</b>	Fe1–N2	1.928(19)
	Fe1–N1	1.967(18)
	Fe1⋯Fe1	11.475
	Fe1⋯Cl1	5.738
<b>2</b>	Fe1–N2	1.946(2)
	Fe1–N1	1.992(2)
	Fe1⋯Fe1	11.388
	Fe1⋯Br1	5.694
<b>3</b>	Fe1–N8	1.947(8)
	Fe1–N2	1.954(8)
	Fe1–N14	1.960(9)
	Fe1–N1	1.973(9)
	Fe1–N7	1.977(9)
	Fe1–N13	1.998(9)
	Fe1⋯Fe1	11.498
	Fe1⋯I1	5.790
<b>4</b>	Fe1–N14	1.948(6)
	Fe1–N8	1.949(6)
	Fe1–N2	1.961(6)
	Fe1–N7	1.981(6)
	Fe1–N13	1.994(6)
	Fe1–N1	1.997(6)
	Fe1⋯Fe1	11.464
	Fe1⋯I1	5.732
<b>5</b>	Fe1–N2	1.960(4)
	Fe1–N14	1.963(4)
	Fe1–N8	1.968(4)
	Fe1–N1	1.998(4)
	Fe1–N13	2.008(4)
	Fe1–N7	2.016(4)
	Fe2–N28	1.958(4)
	Fe2–N34	1.959(4)
	Fe2–N22	1.967(4)
	Fe2–N21	1.994(4)
	Fe2–N27	2.002(4)
	Fe2–N33	2.003(4)
	Fe1⋯Fe2	11.706
	Fe1⋯Cl1	5.863
Fe2⋯Cl1	5.843	

**Table S3.** Hydrogen bonding in the structures of compounds **1-5**.

Compound	D-H...A	D-H (Å)	H...A (Å)	D...A (Å)	D-H...A (°)
<b>1</b>	O1-H1...N6	0.95(2)	2.1(3)	2.94(2)	148(51)
	N4-H4...Cl1	0.88	2.53	3.38(1)	161
	N3-H3B...N5	0.88	2.0	2.78(2)	151
<b>2</b>	O1-H1...N6	0.91(2)	2.09(3)	2.969(4)	163(8)
	N4-H4...Br1	0.88	2.60	3.453(2)	162.6
	N3-H3...N5	0.88	2.01	2.812(4)	150.8
<b>3</b>	N4-H4B...I1	0.88	2.65	3.514(9)	166.5
	N10-H10G...I1	0.88	2.66	3.506(9)	161.3
	N16-H16B...I1	0.88	2.63	3.480(9)	163.4
	N24-H24B...I1	0.88	2.67	3.529(9)	165.1
	N30-H30A...I1	0.88	2.64	3.484(9)	161.6
	N36-H36B...I1	0.88	2.63	3.480(9)	163.2
	N3-H3B...N31	0.88	2.03	2.842(12)	153.2
	N9-H9A...N37	0.88	2.07	2.844(12)	146.1
	N15-H15A...N25	0.88	2.06	2.871(12)	152.3
	N23-H23B...N17	0.88	2.04	2.828(12)	148.1
	N29-H29B...N5	0.88	2.07	2.887(12)	154.0
	N35-H35A...N11	0.88	2.03	2.806(12)	146.2
<b>4</b>	O1-H1-N6	0.90(2)	2.11(3)	2.948(10)	155(7)
	O1-H2-N12	0.90(2)	2.19(4)	3.061(11)	162(13)
	O1-H3-N18	0.90(2)	2.21(4)	3.030(10)	150(8)
	N4-H4B-I1	0.88	2.65	3.498(6)	162.1
	N10-H10B-I1	0.88	2.62	3.467(7)	160.6
	N16-H16B-I1	0.88	2.63	3.471(6)	159.4
	N17-H17-N3	0.88	2.04	2.853(10)	152.2
	N15-H15-N5	0.88	2.07	2.866(10)	149.2
	N11-H11-N9	0.88	2.03	2.855(10)	154.8
	<b>5</b>	N4-H4...Cl1	0.88	2.50	3.351(4)
N10-H10H...Cl1		0.88	2.57	3.419(5)	162.7
N16-H16...Cl1		0.88	2.55	3.410(5)	164.9
N24-H24...Cl1		0.88	2.51	3.359(4)	162.6
N30-H30...Cl1		0.88	2.59	3.445(5)	163.5
N36-H36B...Cl1		0.88	2.53	3.376(5)	161.5
N3-H3...N31		0.88	2.06	2.822(6)	144.9
N9-H9A...N37		0.88	2.02	2.824(6)	151.9
N15-H15A...N25		0.88	2.05	2.834(6)	147.5
N23-H23B...N17		0.88	2.06	2.849(6)	149.4
N29-H29...N5		0.88	2.00	2.798(6)	150.5
N35-H35...N11		0.88	2.01	2.820(6)	153.1

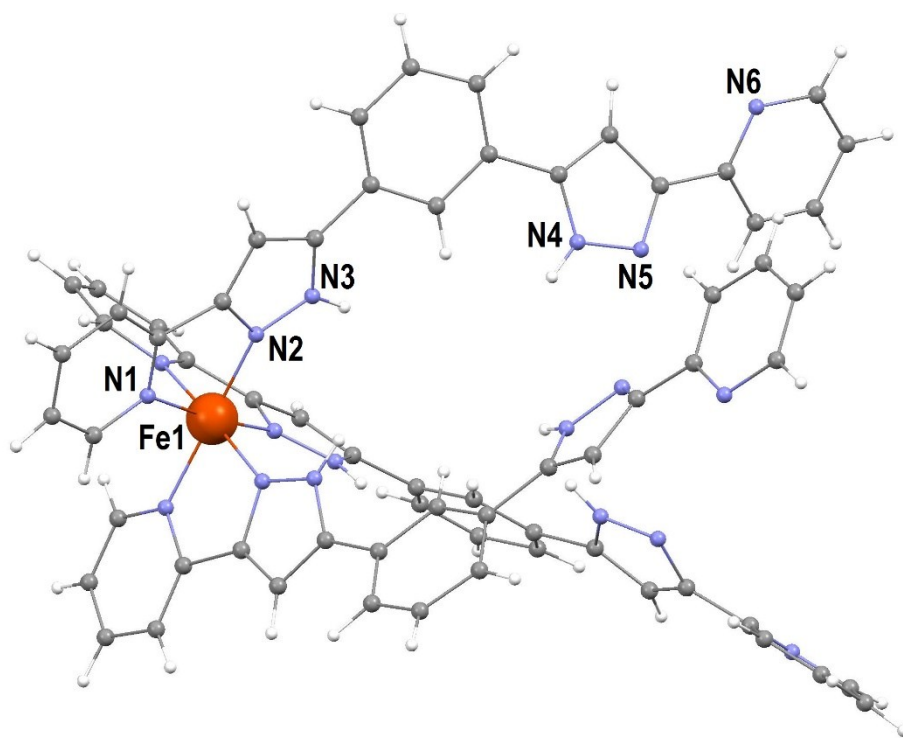


**Figure S1.** Representation of the  $[\text{FeL}_3]^{2+}$  complex within compounds **1** to **5**. Unique heteroatoms of the structure in **1** labelled. Carbon atoms are grey and hydrogen atoms are white.

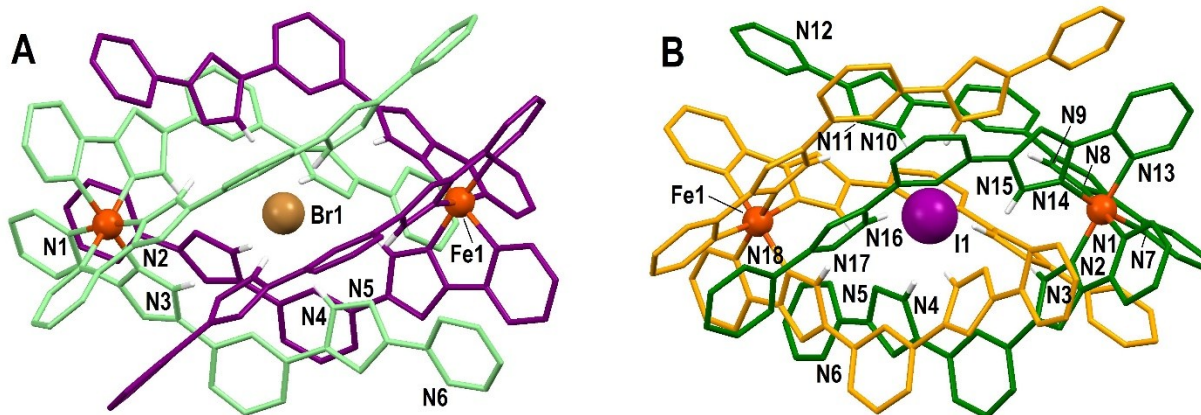


**Figure S2.** Representation of the  $(\text{X}@[FeL_3]_2)^{3+}$  supramolecular assembly in **2** ( $\text{X}=\text{Br}^-$ , A) and in **4** ( $\text{X}=\text{I}^-$ , B). In both cases, the ligands of each  $[FeL_3]^{2+}$  unit are in a different colour. Unique heteroatoms are labelled. Only H atoms of N–H groups are shown (white).

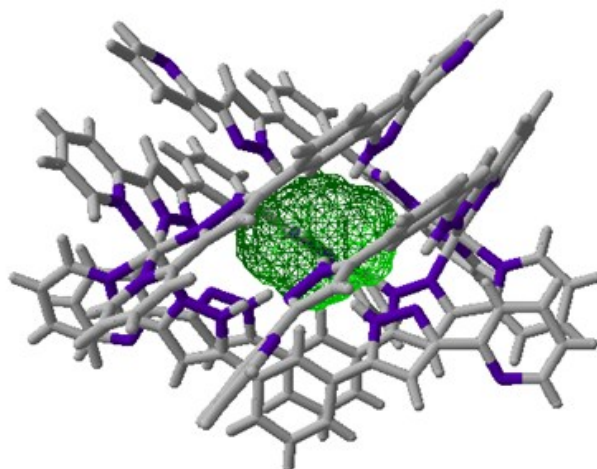


**Figure S3.** Representation of the  $(\text{I}@\text{[FeL}_3\text{]})^{2+}$  host helicate of **3** with the guest removed and the with the volume of the central cavity highlighted as green surface using Swiss-Pdb viewer 4.1 (cavity volume =  $48 \text{ \AA}^3$ ).

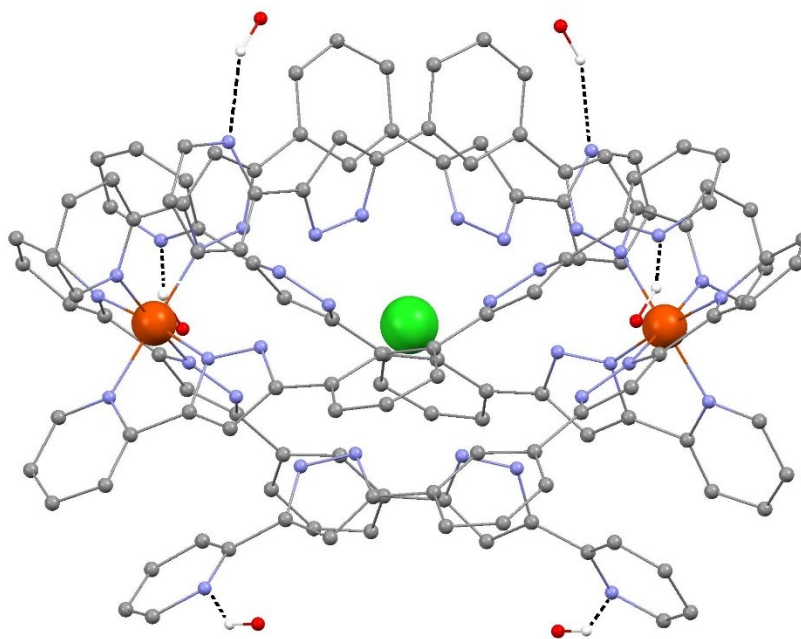


**Figure S4.** Representation of the intermolecular H-bonds between distal pyridine groups of **L** and (disordered)  $\text{H}_2\text{O}$  or  $\text{OH}^-$  moieties in **1**, **2** and **4**.

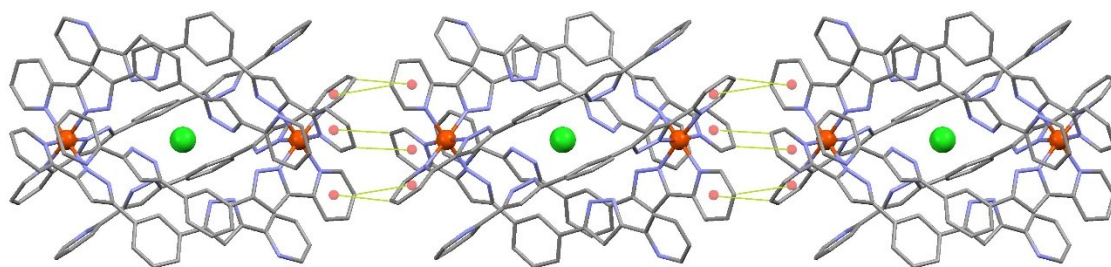


**Figure S5.** Representation of the intermolecular C–H··· $\pi$  interactions between  $(X@[FeL_3]_2)^{3+}$  entities, leading to infinite supramolecular chains in **1**, **2** and **4**.

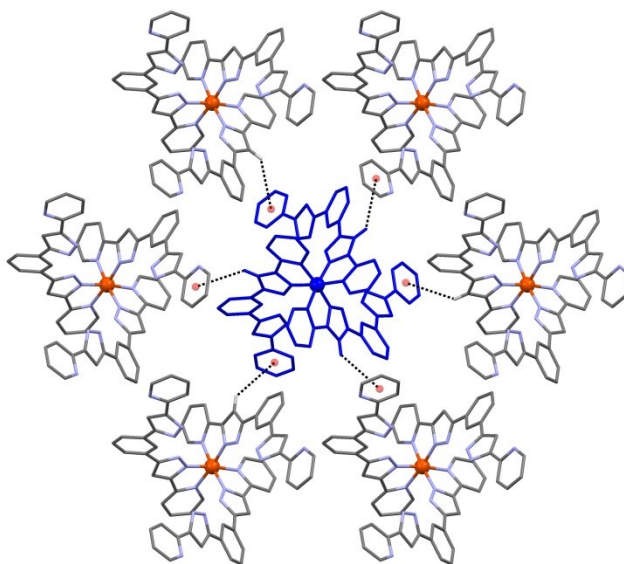


**Figure S6.** Representation of the intermolecular, lateral C–H··· $\pi$  interactions between  $(X@[FeL_3]_2)^{3+}$  entities from parallel supramolecular rods (see Fig. S5) in **1**, **2** and **4**.

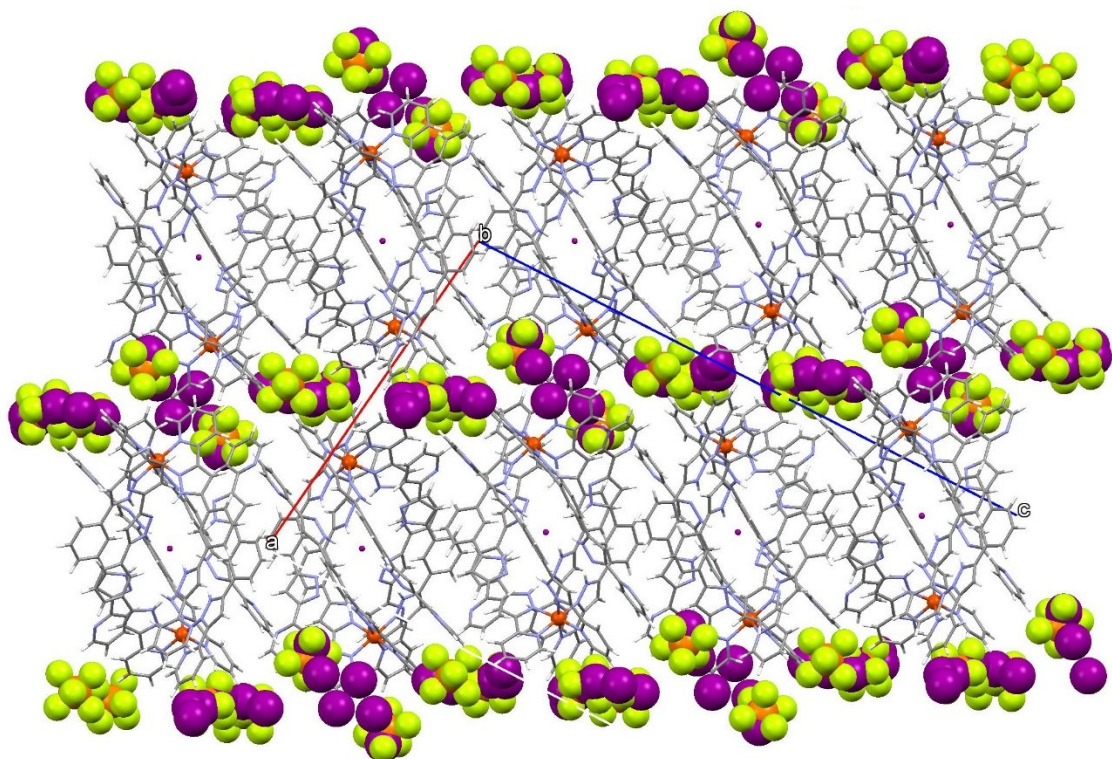


**Figure S7.** Packing diagram of  $(\text{I}@[FeL_3]_2)(PF_6)_{2.23}I_{0.21}(I_3)_{0.56}$  (**3**) down the crystallographic  $b$  axis, emphasizing the alternation of “hydrophobic sheets” containing the largely organic  $(\text{I}@[FeL_3]_2)^{3+}$  moieties (represented as grey and white capped sticks) and “hydrophilic layers” formed by external counter-ions consisting in  $PF_6^-$ ,  $I^-$  and  $I_3^-$  groups, represented as green (F), orange (P) or purple (I) balls.

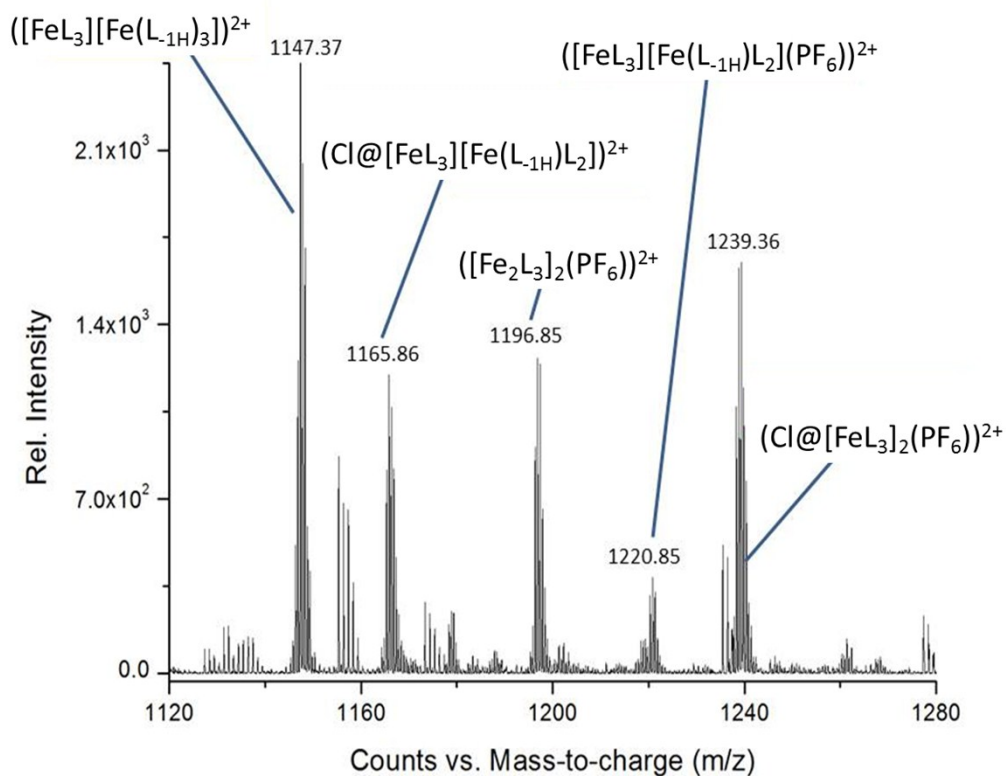
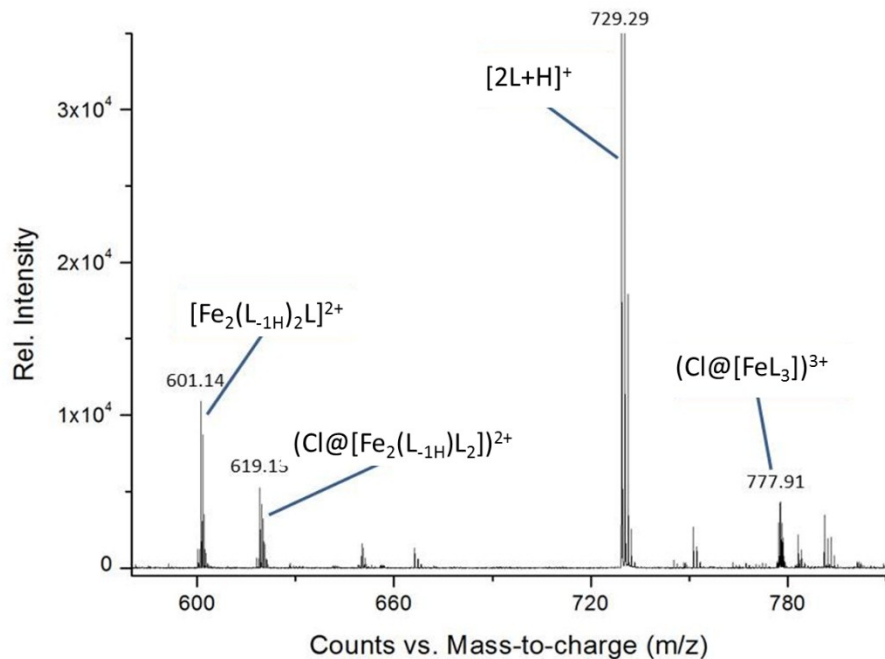


**Figure S8.** ESI<sup>+</sup>-MS spectrograms of **1** in various regions. Peaks related to the  $(\text{Cl}@\text{Fe}_2\text{L}_3)^{3+}$ ,  $(\text{Cl}@\text{FeL}_3)_2^{3+}$ ,  $[\text{Fe}_2\text{L}_3]^{4+}$  and  $([\text{FeL}_3]_2)^{4+}$  assemblies are found.

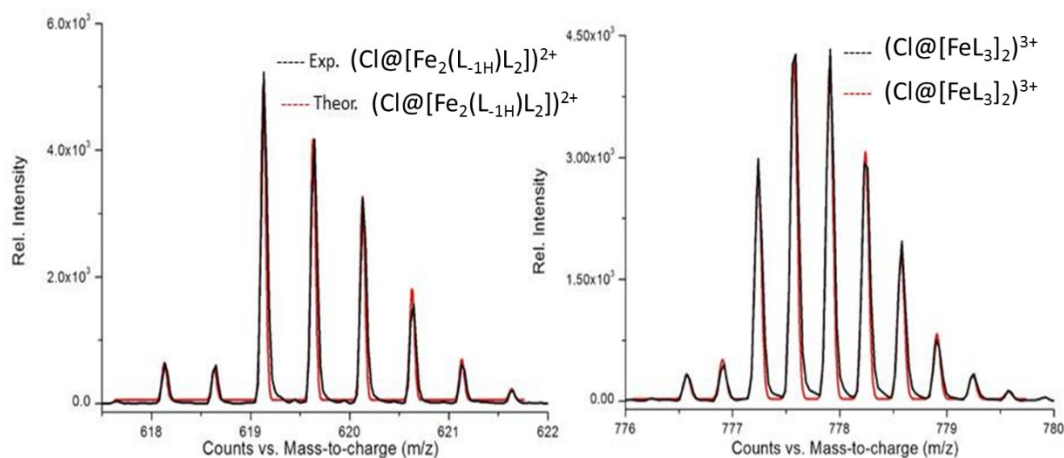


**Figure S9.** Detail and simulation of the signals related to the  $(\text{Cl}@[Fe_2L_3])^{3+}$  (left) and  $(\text{Cl}@[FeL_3]_2)^{3+}$  (right) fragments of **1**, showing the expected multiplets for the isotopic distribution.

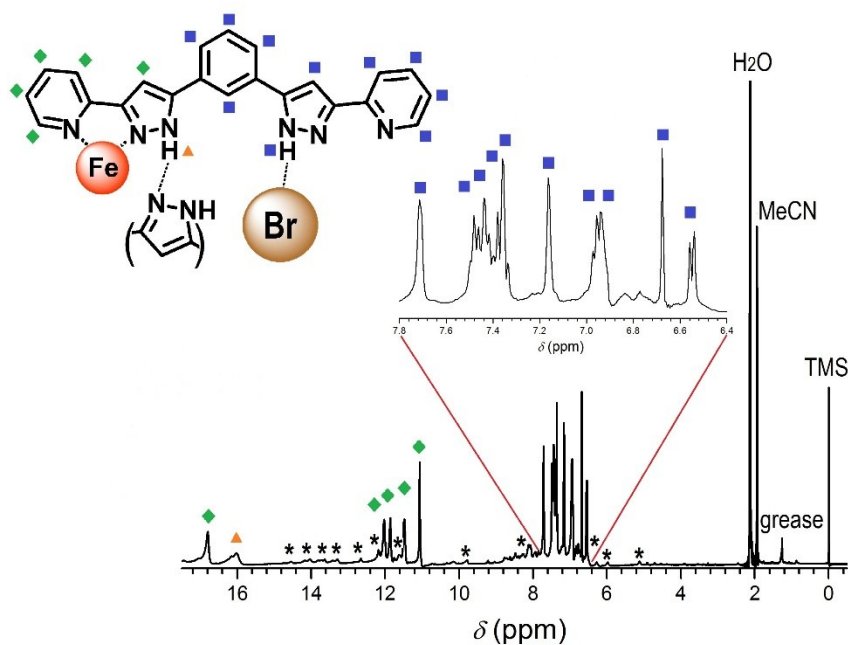


**Figure S10.**  $^1\text{H}$  NMR spectrum of **2** in  $d_3$ -MeCN at room temperature, evidencing the stability of the  $(\text{Br}@[FeL_3]_2)^{3+}$  species in solution. The asterisks correspond very minor and related supramolecular species (see text).

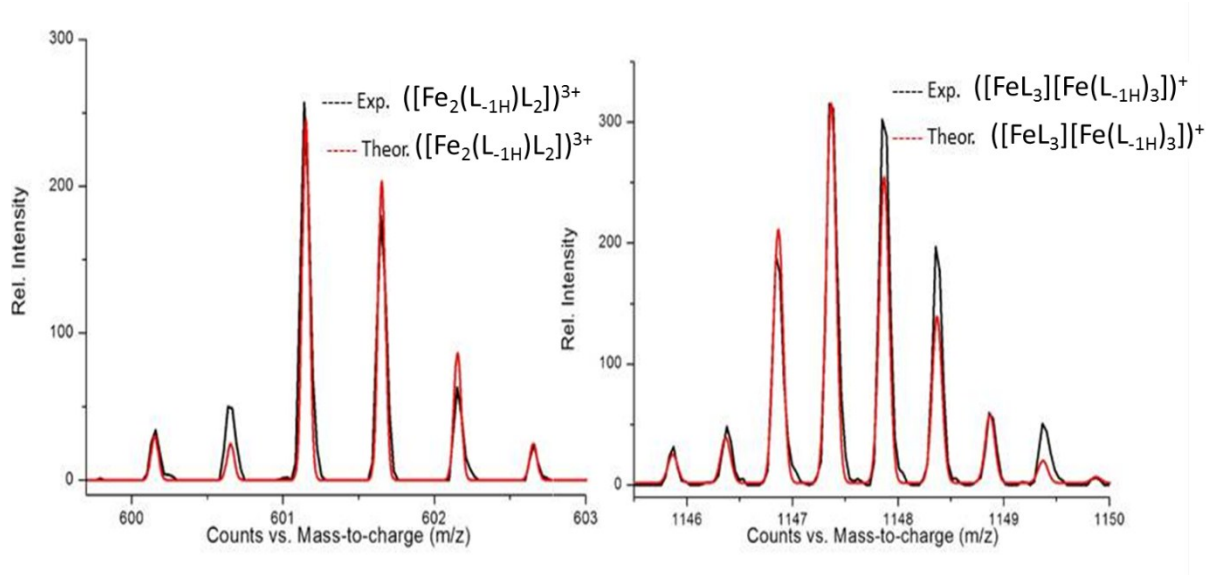


**Figure S11.** Detail and simulation of the signals related to the  $[\text{Fe}_2\text{L}_3]^{4+}$  (left) and  $([\text{FeL}_3]_2)^{4+}$  (right) fragments in **2** (see text), showing the expected multiplets for the isotopic distribution.

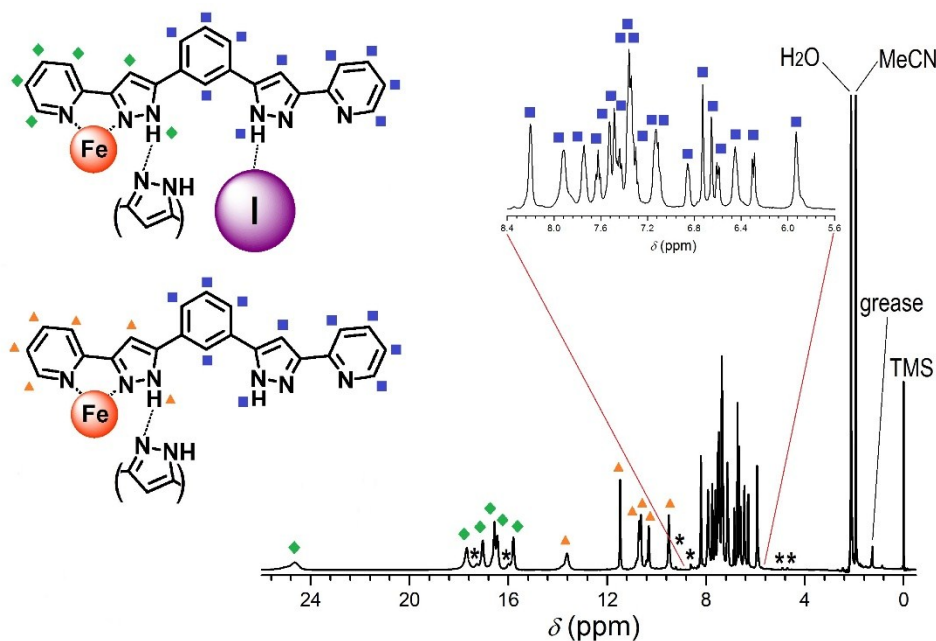


**Figure S12.**  $^1\text{H}$  NMR spectrum of **3** in  $d_3$ -MeCN at room temperature, evidencing the equilibrium between of the  $(\text{I}@\text{[FeL}_3]_2)^{3+}$  and the  $([\text{FeL}_3]_2)^{4+}$  species in solution. The asterisks correspond very minor and related supramolecular species (see text).